

0947

Improved parallel imaging with N-periodic spatial banding patterns in bSSFP

Zimu Huo^{1,2}, Lorena Garcia-Foncillas¹, Krithika Balaji¹, Michael Mendoza¹, Neal K Bangerter¹, and Peter J Lally¹
¹Imperial College London, London, United Kingdom, ²University of Cambridge, Cambridge, United Kingdom

Synopsis

Keywords: Parallel Imaging, Parallel Imaging

Motivation: This research explores the potential for temporally varying N-periodic bSSFP banding artifacts as a new dimension alongside coils for parallel imaging.

Goal(s): Our goal is to leverage the temporally varying spatial modulation of a 2-periodic bSSFP acquisition to improve parallel imaging performance over a straightforward bSSFP approach.

Approach: We optimize imaging parameters using computational simulations and validate our methodology through in-vivo experiments in brain.

Results: Our findings demonstrate that the banding artifacts from 2-periodic bSSFP can serve as additional spatial encoding information in parallel imaging applications to reduce scan time.

Impact: Periodically varying bSSFP banding patterns can be exploited to achieve improved parallel imaging performance, creating opportunities for new experimental designs in accelerated imaging.

Introduction

Balanced steady-state free precession (bSSFP) is widely used due to its high signal-to-noise ratio (SNR) efficiency¹. However, its signal is strongly dependent on local off-resonance, and so in regions with large B_0 field inhomogeneity this results in undesirable banding artifacts. Via linear RF phase-cycling, these patterns can be shifted across several acquisitions, which can then be combined to generate band-free images. In each of these bSSFP acquisitions the signal is therefore spatially modulated by both the coil sensitivity and bSSFP spectral profiles²⁻³. These undesirable banding artifacts can be considered as useful encoding information, offering the potential for greater acceleration factors while maintaining image fidelity. Instead of linear phase-cycling, quadratic phase-cycling in bSSFP creates alternating equilibrium magnetization, producing to N-periodic bSSFP⁹. This offers a new dimension for parallel imaging reconstruction. In this work, we show 2-periodic bSSFP (FEMR⁸⁻⁹) acquisitions can outperform linear RF phase-cycled bSSFP in parallel imaging applications, allowing for greater acceleration.

Theory

In the context of the Super Field-of-View (sFOV) framework², it is possible to interpret bSSFP banding patterns as sensitivity profiles similar to the ones used in parallel imaging. In this setting, the k-space signal S obtained from the n-th acquisition at spatial location r can be expressed as:

$$S_n = F\{C_n(r)M_s(r)\}$$

where C denotes the bSSFP profile modulation, M denotes the magnetization, and F denotes the Fourier transform operator. Assuming data are acquired with a single coil receiver, the bSSFP spatial profiles can be estimated based on fully sampled central k-space data⁴⁻⁵. As such, these profiles may serve as spatial encoding to address an inverse problem that seeks to recover aliased data from a collection of under-sampled linear RF phase-cycled bSSFP images. The theoretical upper limit for acceleration factor is frequently unachievable in practical settings due to the presence of overlapping coil sensitivity profiles⁶. In this work, we propose the application of a quadratic RF phase-cycling of 180° to the standard bSSFP sequence, resulting in the generation of a 2-periodic bSSFP acquisition called FEMR⁸⁻⁹ (Figure 1). As shown in Figure 2, the more orthogonal 2-periodic FEMR profiles resulting from quadratic RF phase-cycling can be used to better condition the inverse reconstruction problem.

Methods

We first performed a Bloch simulation to optimize the imaging parameters and phase cycle combination methods¹. The weighted-combination SSFP (WC-SSFP) approach is explored to produce uniform and high SNR images in brain applications⁷. Assuming there are N separate bSSFP images, the combined images Y can be expressed as:

$$Y = \left| \sum_{n=1}^N |X_n|^p X_n \right|^{\frac{1}{p+1}}$$

where X_n denotes the image from n-th acquisition. The combination norm p controls the trade-off between SNR and ripples. To validate our approach, we conducted an in-vivo acquisition experiment utilizing a 3T Siemens MAGNETOM Verio (Erlangen, Germany) scanner from 3 healthy subjects. 8 linear phased-cycled bSSFP images ($\Delta\phi_{\text{linear}} = 0^\circ, 45^\circ, 90^\circ, 135^\circ, 180^\circ, 225^\circ, 270^\circ, 315^\circ$) and 4 linear phased-cycled FEMR images ($\Delta\phi_{\text{quad}} = 180^\circ$; $\Delta\phi_{\text{linear}} = 0^\circ, 45^\circ, 90^\circ, 135^\circ$) were acquired. These images were acquired from a 2D axial slice through the head, with a spatial resolution of $1.0 \times 1.0 \times 5.0$ mm and a field-of-view of 250 mm. The imaging parameters were set as follows: TR=8.6ms, TE=4ms, and $\alpha = 30^\circ$, with a bandwidth of 224Hz/px. The FEMR flip angle was set to 25° . Parameter choices for both bSSFP and FEMR acquisitions were chosen based on the Bloch simulations (see Results section). The data were undersampled regularly in 1D by four factors: 2,4,6,8. We reconstructed the data using GRAPPA with kernel size 4x5. The optimal value of Tikhonov regularization parameter was found using a parameter sweep between $\lambda \in \{0, 1e^{-15}\}$ for both bSSFP and FEMR.

Results

Bloch simulations recommended a 30° flip angle and a combination norm of 2 for bSSFP, while FEMR results indicated a 25° flip angle and the same combination norm of 2. For the in-vivo data, the statistical analysis was conducted utilizing pairwise comparisons between sequence across a range of undersampling ratios (Figure 5). The in-vivo results indicated a significant improvement in reconstructed image quality using the FEMR.

Discussion

The optimal choice of flip angle and N-periodicity will depend on the specific application. Profile encoding methods rely on smooth B_0 field variations for spatial encoding and rapid profile changes can lead to suboptimal reconstruction results. To address this, it is necessary to expand the auto-calibration region to capture high-frequency information and enlarge the interpolation kernel.

Conclusion

In this work, we have shown that an N-periodic bSSFP acquisition can provide additional spatiotemporal sensitivity profiles which improve the performance of parallel imaging reconstructions over linear RF phase-cycled bSSFP. The encoding is independent of the coil geometry profile, and provides new opportunities for experimental design in accelerated imaging.

Acknowledgements

We acknowledge generous support from The Wellcome Trust (220473/Z/20/Z), The Edmond J Safra Foundation, UK Dementia Research Institute, NIHR Imperial Biomedical Research Centre, and National Institutes of Health (R01EB002524).

References

1. Neal K. Bangerter, Brian A. Hargreaves, Shreyas S. Vasanaawala, John M. Pauly, Garry E. Gold, and Dwight G. Nishimura. Analysis of multiple-acquisition SSFP. *Magnetic Resonance in Medicine*, 51(5):1038–1047, 2004.2
2. Michael Lustig. et al. A Super-FOV method for rapid SSFP banding artifact reduction. *ISMRM*, 2005.3
3. Erdem Biyik, Efe Ilicak, and Tolga C. ukur. Reconstruction by calibration over tensors for multi-coil multi-acquisition balanced SSFP imaging. *Magnetic Resonance in Medicine*, 79(5):2542–2554, September 2017.4
4. Mark A. Griswold, Peter M. Jakob, Robin M. Heidemann, Mathias Nittka, Vladimir Jellus, Jianmin Wang, Berthold Kiefer, and Axel Haase. Generalized autocalibrating partially parallel acquisitions (GRAPPA). *Magnetic Resonance in Medicine*, 47(6):1202–1210, June 2002.5
5. Klaas P. Pruessmann, Markus Weiger, Markus B. Scheidegger, and Peter Boesiger. SENSE: Sensitivity en-coding for fast MRI. *Magnetic Resonance in Medicine*, 42(5):952–962, November 1999.6
6. Jesse Hamilton, Dominique Franson, and Nicole Seiberlich. Recent advances in parallel imaging for MRI. *Progress in Nuclear Magnetic Resonance Spectroscopy*, 101:71–95, August 2017.7
7. Tolga C. ukur, Neal K. Bangerter, and Dwight G. Nishimura. Enhanced spectral shaping in steady-state freeprecession imaging. *Magnetic Resonance in Medicine*, 58(6):1216–1223, 2007.7
8. Vasanaawala SS, Pauly JM, Nishimura DG. Fluctuating equilibrium MRI. *Magn Reson Med*. 1999 Nov;42(5):876–83. doi: 10.1002/(sici)1522-2594(199911)42:5<876::aid-mrm6>3.0.co;2-z. PMID: 10542345.
9. Peter J Lally, Mark Chiew, Paul M Matthews, Karla L Miller, and Neal K Bangerter. A Motion-Robust, Short-TR Alternative to Multi-Echo SPGR. *ISMRM Workshop on Data Sampling & Image Reconstruction 2023*

Figures

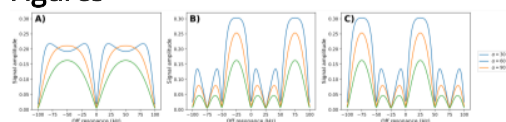


Figure 1: Equilibrium transverse magnetization versus off-resonance profiles of bSSFP sequences. The FEMR profile is determined by two key parameters: a linear phase cycle term, which governs the shift between acquisitions, and a quadratic phase cycle term of 180 degrees, which regulates the profile shift per TR. The signal magnitude is shown at TE = TR/2 for species with T1 = 1000 ms, T2 = 200 ms, and TR = 10 ms. Figure A) shows bSSFP spectra for various flip angles. Figures B) and C) show the FEMR echoes acquired after even and odd excitations for a single acquisition.

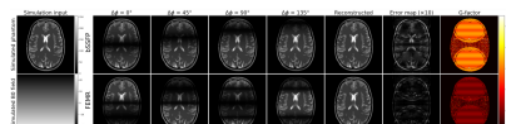


Figure 2: Outline of sFOV Theory with simulated phantom. The images from standard bSSFP and FEMR acquisitions are undersampled and reconstructed using a separate calibration signal in the center of k-space. The 4-phase cycled FEMR exhibited superior performance over the 8-phase cycled bSSFP, with a 52 % reduction in RMSE and a 15 % decrease in average g-factor. This result was expected due to the highly orthogonal profiles produced by the FEMR method.

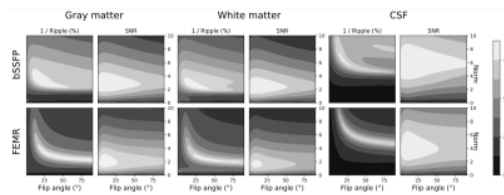


Figure 3: The percent ripple and SNR efficiency of bSSFP and FEMR for gray matter, white matter, and CSF. The inverse of percent ripple and SNR are normalized between 0 to 100 while preserving the same relative ratio between the bSSFP and FEMR for each tissue type. The bright region in this contour plot corresponds to the desired parameters. The tissue parameters are as follows: white matter (T1: 780 ms, T2: 60 ms), gray matter (T1: 920 ms, T2: 100 ms), and cerebrospinal fluid (T1: 4000 ms, T2: 2000 ms).

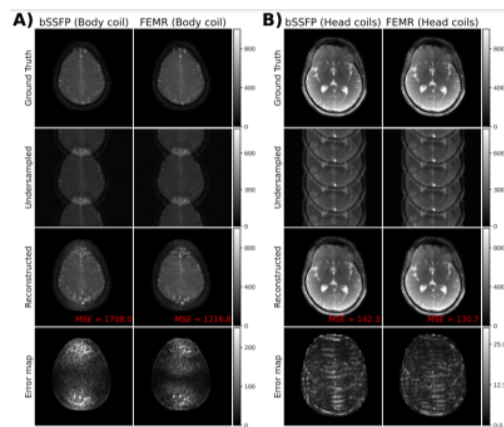


Figure 4: An example GRAPPA reconstruction for 8 phase cycled bSSFP and 4 phase cycled FEMR. The left part shows the acquisition with an inbuilt single-channel body receive coil with undersample ratio of 2. The right part shows the acquisition with 32 channel head-coil with undersampling ratio of 4. The undersampling ratio is chosen to best reflect the difference between the bSSFP and FEMR for their respective scenarios.

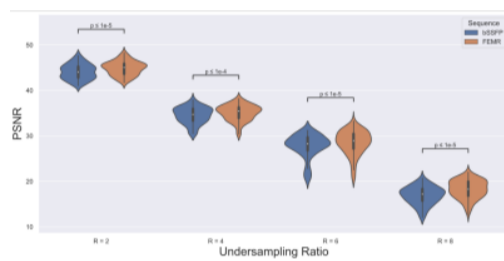


Figure 5: The PSNR values for different acceleration factors. FEMR technique consistently outperforms bSSFP, especially at higher acceleration factors.